Exciton–plasma crossover with electron–hole density in T-shaped quantum wires studied by photoluminescence spectrograph method

Masahiro Yoshita, Yuhei Hayamizu, and Hidefumi Akiyama*
Institute for Solid State Physics, University of Tokyo, and CREST, JST
5-1-5 Kashiwanoha, Kashiwa, Chiba 277-8581, Japan

Loren N. Pfeiffer and Ken W. West
Bell Laboratories, Lucent Technologies,
600 Mountain Avenue, Murray Hill, NJ 07974
(Dated: 9/5)

We investigated the evolution of photoluminescence (PL) spectra with the electron–hole (e–h) pair density in a single T-shaped quantum wire of high quality grown by a cleaved-edge overgrowth method with molecular-beam epitaxy. By using a spectrograph imaging method for the PL measurements, we obtained PL spectra free from carrier migration effects for the one-dimensional (1D) e–h system in the T wire for a wide range of e–h pair densities from 5×10^1 to 1.2×10^6 cm^{-1}. In the low e–h pair density region below 4×10^3 cm^{-1}, PL only from 1D excitons in the wire was observed. At a pair density of 4×10^3 cm^{-1}, a new peak characteristic of biexcitons with a binding energy of 2.8 meV appeared below the exciton peak. At a pair density of 1×10^5 cm^{-1}, the biexciton peak started broadening without a peak energy shift and completely changed to an e–h plasma at 6×10^5 cm^{-1}. The transition from the dilute exciton gas to the e–h plasma is, therefore, a gradual crossover via biexcitons, which indicates the importance of biexcitonic effects in 1D e–h systems. Moreover, we found that during the continuous exciton–plasma crossover, the band edge of 1D excitons showed no significant energy shift at an e–h pair density as high as 2×10^5 cm^{-1}, where the biexciton PL peak had already started broadening in linewidth and changing to the degenerate e–h plasma peak. The level crossing between the band edge and the exciton was not observed experimentally.

I. INTRODUCTION

Many-body effects in optically excited semiconductors, which play essential roles in the crossover from an exciton gas at low electron–hole (e–h) pair densities to a dense e–h state (e.g., an e–h plasma) at high densities, have attracted much attention and have been actively studied experimentally and theoretically.[1,2] Recently, intensive interest has been focused on one-dimensional (1D) e–h systems in semiconductor quantum wires, where Coulomb interactions become more important.[3–16]. In three-dimensional (3D) e–h systems, it is accepted that the exciton–plasma transition with the carrier density is well described by a familiar picture of exciton Mott transition. In this picture, the binding energy of excitons decreases with carrier density due to screening, and the Mott transition to the e–h plasma occurs at the critical density n_c (the Mott density) where the exciton binding energy is reduced to zero and the energy position of the band edge coincides with that of the excitons.[17] However, in 1D e–h systems, the validity of the exciton Mott transition picture is still questionable because the screening effect, which is a key factor in this picture, becomes much weaker in lower-dimensional systems.[18–20] Indeed, a many-body theory shows that optical spectra for quasi-1D systems calculated for various carrier densities with and without screening effects are almost identical,[21] indicating that the screening effects are less important in the exciton–plasma crossover in quasi-1D systems.[1] Furthermore, it is known that any weak attractive potential forms at least one bound state in 1D. The 1D exciton Mott transition picture includes these crucial problems.

Experimental studies[9,10] on many-body effects for semiconductor quantum wires reported that photoluminescence (PL) peak positions of excitons in the quantum wires are almost independent of the e–h pair densities up to a very high carrier density of 3×10^6 cm^{-1}. Recent many-body theories explain this constancy of the exciton peak positions qualitatively as an exact cancellation between the reduction in the exciton binding energy and the shrinkage of the band gap due to band-gap renormalization.[7] However, quantitative comparisons of experimental data with theories have not been achieved yet. Moreover, the crucial energy shift of the band edge and the reduction of the exciton binding energy have not been directly measured. To solve these problems and establish a picture for the 1D exciton–plasma crossover, quantitative systematic experiments are necessary.

In practical experiments on low-dimensional systems formed in hetero-structures, interface roughness and the resulting localization of the electronic states are crucial issues.[22,23] If structural roughness is large, carriers are localized and zero-dimensional (0D) states are formed. Indeed, localized states formed in thin two-dimensional (2D) quantum wells with large interface roughness have been used to study 0D quantum-dot features[24–26] as those realized in self-assembled InAs quantum dots.[27] In such systems, 0D states show sharp PL peaks with radiative-relaxation widths due to 0D excitons, biexcitons, and other neutral exciton complexes, which do not

shift with carrier densities as a result of 3D confinement. Detailed PL studies on previous T-shaped quantum wires (T wires) formed by a cleaved-edge overgrowth method have revealed 0D-like localized electronic states in the T wires.[23,28] Therefore, for investigations of the intrinsic 1D problems in the exciton–plasma crossover at low temperatures, it is important to minimize structural roughness in order to get small inhomogeneous PL linewidth and localization energy, at least smaller than the many-body Coulomb interaction energies such as exciton and biexciton binding energies.

Recently, the structural uniformity of T wires has been significantly improved. In our 20-period multiple T-wire laser samples, the 1D-exciton ground state and 1D continuum states were spectrally separated,[29,30] and PL peaks of excitons, biexcitons, and an e–h plasma were found as well as laser emissions.[16] Further improvements in structural uniformity and spectral sharpness were achieved in single T-wire laser samples, where we observed single-mode lasing[31,32] and sharp strong exciton photoabsorption in a waveguide-transmission measurement.[33]

In this paper, we describe our first quantitative PL studies on the single T wire with the current-best quality, whose inhomogeneous broadening is smaller than the relevant Coulomb interaction energies under investigation. In particular, we studied the evolution of PL shape, energy, and intensity during the crossover from dilute 1D excitons to a dense e–h plasma as a function of well-characterized e–h density.

In high-quality quantum wires with reduced interface roughness, the migration of carriers (electrons, holes, and excitons) is enhanced. In micro-PL experiments, this enhanced carrier migration causes spatial gradation of carrier densities in the wire, which leads to the obtained PL spectra of the wire becoming average spectra from various e–h density regions. To reduce this averaging effect in the spectra, in this work we used a spectrograph imaging method for micro-PL measurements and derived PL spectra of the wire free from the carrier migration. In addition, we estimated carrier densities in the wire at each excitation power by comparing PL intensities to that obtained at the saturated carrier density in the wire. These improvements in experiments enable quantitative discussion of the spectral evolution of PL from the wire with the carrier density.

This paper is organized as follows. In the next section, we describe the single T-wire sample structure and micro-PL experimental setup combined with the spectrograph method. In Sec. III.A, we characterize the spatial uniformity and quality of the single T wire by scanning micro-PL spectroscopy. Then, in Sec. III.B, we report spectrograph PL imaging experiments for the single T wire at various excitation powers. We demonstrate spectrograph PL images that are strongly dependent on the excitation power and show significant carrier migration in the wire. In Secs. III.C-E, we derive intrinsic PL spectra from the spectrograph images for various e–h densities. We focus on PL from the ground state of 1D excitons and from the 1D continuum states in the wire and discuss their spectral evolution as a function of the 1D carrier density. Finally, in Sec. IV, we discuss problems of the exciton Mott picture in the 1D e–h system of the wire by comparing the obtained experimental results with theoretical predictions based on the exciton Mott transition picture.

II. EXPERIMENT

A. Sample preparation

A single T wire was fabricated by the cleaved-edge overgrowth method with molecular beam epitaxy[34,35] with a growth-interrupt *in-situ* annealing technique.[36,37] As schematically illustrated in Fig. 1(a), the single T wire consisted of a 14-nm-thick $Al_{0.07}Ga_{0.93}As$ quantum well (QW) (stem well) grown on a (001) substrate and an intersecting 6-nm-thick GaAs QW (arm well) overgrown on a cleaved (110) edge of the stem well. We improved the interface flatness of the arm well by performing growth-interrupt *in-situ* annealing at a substrate temperature of 600°C for 10 minutes on the arm-well upper surface.[36,37] The sample structure and fabrication procedures are reported in detail in separate papers.[31,32]

B. Micro-PL experiments combined with spectrograph imaging method

The micro-PL setup used in this study is schematically shown in Fig. 1(b). For photoexcitation, light from a titanium-sapphire laser was focused, via an objective lens with a numerical aperture (NA) of 0.5, to an almost-diffraction-limited spot with a diameter of 0.8 μm on the sample surface.[38] For PL detection, we used a spectrographic technique with an imaging monochromator and a liquid-nitrogen-cooled charge-coupled-device (CCD) camera with 1024×256 pixels. PL from the sample was collected by the objective lens and projected onto the entrance slit of the monochromator via an imaging lens. Then, the PL images were dispersed in wavelength by the monochromator and detected by the CCD camera.

In the experiments, we projected the PL images on the slit with the wire direction aligned parallel to the slit, as illustrated in Fig. 1(b), so that the spatial distribution of PL and hence the spatial distribution of photoexcited carriers in the wire could be observed directly. In addition, by extracting a specific row of the dispersed PL image detected by the CCD camera, we obtained a spatially resolved PL spectrum of the wire at the corresponding sample position. In particular, the PL spectrum extracted at the excitation position of the laser corresponds to the spectrum obtained in the confocal micro-spectroscopy experiments.

The spatial resolution of the spectrograph image along the wire direction was about 0.8 μm on the sample, which is determined by the NA (= 0.5) of the objective lens, the magnification factor (×32) of the micro-PL detection system, and the pixel size (24μm × 24μm) of the CCD camera. The spatial resolution across the wire direction was also determined by these values in the micro-PL detection system mentioned above and by the slit width of the monochromator. In this study, the slit width was set to 25 μm, which limited the detection area to about 0.8 μm on the sample across the wire direction and gave a spectral resolution of 0.1 nm.

III. RESULTS

A. Spatial uniformity of the T wire

Figure 2 shows spatially resolved PL spectra of the single T wire at 5 K obtained by scanning the 0.8-μm-diameter excitation spot along the wire in steps of 0.5 μm over a distance of 15 μm. The photon energy of the excitation laser was 1.691 eV and the excitation power was as low as 4 nW on the sample surface. PL peaks observed around 1.582 and 1.636 eV are ascribed to the wire and the stem well, respectively, on the basis of a separate PL imaging experiment.[32] PL from the arm well was not observed due to the fast flow of carriers from the arm well to the wire.

The dominant PL peak from the wire at 1.582 eV had a narrow linewidth of 1.3 meV and uniform peak intensity and energy. This peak has been ascribed to the ground state of the 1D excitons in the wire with a small Stokes shift of less than 0.3 meV.[29,30,33] Tiny PL peaks locally observed at 1.580 eV are from 1D excitons in the wire formed in the arm-well monolayer-island regions.[37] However, as seen in Fig. 2, these monolayer fluctuations are rare in the constituent arm well and a continuous sequence of wire PL spectra was obtained, which demonstrates that the spatially uniform 1D exciton states were formed over a region at least 10 μm in length in the wire. Scanning PL experiments over the entire sample have confirmed that the whole 500-μm-long wire has features very similar to Fig. 2.

B. Spectrograph images of PL from the T wire

Spectrograph images of PL from the single T wire observed at three different excitation powers (0.16 μW, 21.6 μW, and 0.35 mW) are shown in Fig. 3. The excitation position was selected at the center of the spatially uniform PL region in Fig. 2. The photon energy of the excitation laser was 1.6146 eV. This excitation created e–h pairs in the T wire and the arm well, but not in the stem well. The horizontal and vertical axes of the images represent photon energy and spatial distance from the excitation position on the sample, respectively. Tiny spots seen at 1.6146 eV are reflection images of the excitation laser spot. Their image sizes along the wire direction are almost 1 pixel of the CCD, which ensures that the spot size of the excitation laser was 0.8 μm or less on the sample surface.

In Fig. 3, the PL images strongly depend on the excitation power. The PLs of the wire and the arm well were observed from regions widely spread along the wire direction from the excitation position. In particular, at the highest excitation power of 0.35 mW, strong PL was observed even at positions 10 μm away from the excitation position, which indicates the existence of significant carrier migration in the wire. In addition, the spectral linewidth of the wire PL increased as the excitation power was increased.

Figure 4(a) shows PL spectra at every 4-μm step from the excitation position (d = 0 μm), extracted from the spectrograph image for 0.35-mW excitation power in Fig. 3. For comparison, the PL spectrum integrated over all the rows of the spectrograph image along the wire direction is shown in Fig. 4(b). The PL spectra of the wire strongly depended on the detection position because of significant carrier migration in the wire. The spectrum at the excitation position (d = 0 μm) has a broad single-peak structure, while those at the positions far from the excitation spot (d = ±8 μm) have a double peak structure. Figure 4(c) shows the PL intensity profile along the wire, obtained by summing the PL intensities of the wire between 780 and 790 nm. This intensity profile indicates that the photogenerated carriers were spatially extended over a distance of 10 μm along the wire direction, and relatively strong PL was observed at positions 5-μm from the laser excitation position. As a consequence, the integrated PL spectrum shown in Fig. 4(b), which corresponds to the spectrum obtained in a conventional micro-PL measurement without using the spectrograph technique or confocal micro-spectroscopy, does not represent an intrinsic PL spectrum of the wire at a defined carrier density but shows only a mixed PL spectrum of the wire under a larger spatial distribution of carriers. Therefore, we extracted PL spectra at the excitation position from the spectrograph images to eliminate the influence of carrier migration along the wire direction on the PL spectra and compared them at various excitation powers. Since the carrier migration length was larger than the spatial resolution and the laser spot size of 0.8 μm, the carrier-distribution effects were negligible in the extracted PL spectra.

C. Excitation-power dependence of PL spectra and evaluation of the e–h density

Figure 5 shows PL spectra of the T wire at the center position of the excitation spot for various excitation powers (P_{ex}) at 5 K, derived from the spectrograph images. At excitation powers less than 0.1 μW, only a single PL peak due to 1D excitons of the wire was observed at

1.582 eV. As the excitation power was increased from 0.1 μW to around 10 μW, a new PL peak (labeled the S-peak) appeared 2.8 meV below the exciton PL peak and increased in intensity rapidly. Above 10 μW the S-peak dominated the PL of the wire as its linewidth broadened. Above 50 μW the exciton peak faded into the high-energy tail of the S-peak. The dominant S-peak finally showed a red-shift and an asymmetric shape. Simultaneously, PL peaks from the arm well observed at 1.603 and 1.608 eV strongly increased in intensity.

Integrated area intensities (the sum of the exciton- and S-peak intensities) of the wire PL spectra and those of the arm-well PL spectra are plotted in Fig. 6. The PL intensity of the wire became saturated at an excitation power of about 0.2 mW while that of the arm well still increased. This indicates that the electronic states in the wire were completely filled and the Fermi filling of the arm well had started.

The saturation density of the e–h pairs in the wire, estimated from the 21-meV energy separation between the ground states of the wire and the arm well in this T-wire sample, was 1.2×10^6 cm^{-1}. By assuming that the PL intensity is proportional to the e–h pair density (n_{1D}) in the wire, we estimated n_{1D} for each PL spectrum, which is shown in parentheses under the P_{ex} in Fig. 5. In the following sections, we use the estimated 1D e–h pair density n_{1D} to discuss the spectral evolution quantitatively.

D. PL of excitons, biexcitons, and an e–h plasma in the T wire

Figure 7(a) shows the PL intensities of the wire and the arm well plotted as a function of the estimated 1D e–h pair densities n_{1D}. PL intensities of the exciton and the S-peak constituting the wire PL are also shown. The PL intensity of the wire was saturated at n_{1D} of 1.2×10^6 cm^{-1} while that of the arm well increased.

At carrier densities below 4×10^3 cm^{-1}, only the PL peak from excitons in the wire had a measurable intensity. Above 4×10^3 cm^{-1}, however, the S-peak appeared and increased in intensity steeply (Fig. 7(a)). Log-log plots of the integrated intensity of the S-peak against that of the exciton peak are shown in Fig. 7(b). The S-peak intensity increased superlinearly against the exciton peak intensity, and the slope gradually approached 2. Peak energy positions and linewidths (FWHM) of these two peaks are shown as a function of n_{1D} in the upper and lower panels of Fig. 8, respectively. The energy position and the linewidth of the S-peak and the exciton peak were almost unchanged in the 1D e–h pair densities between 4×10^3 cm^{-1} and about 1×10^5 cm^{-1} (Fig. 8). In addition, these two peaks come from the same position in the wire at the excitation spot. Therefore, we ascribe the S-peak in this density region to a dilute gas of biexcitons. The corresponding mean distances r_s between carriers are $200a_B^*$ and $8a_B^*$, respectively, where a_B^* (=12.7 nm) is the Bohr radius of bulk GaAs. These values are reasonable for the formation of biexcitons. The biexciton binding energy estimated from the PL spectra was 2.8 meV, which is in agreement with our previous result for multiple T wires.[16]

In the high density region above n_{1D} of 1×10^5 cm^{-1}, the linewidth of the S-peak increased significantly from 2 to 12 meV with the excitation power (bottom panel of Fig. 8). The linewidth of the exciton peak also increased with the excitation power, but its intensity was saturated at 6×10^5 cm^{-1} and then rapidly decreased (Fig. 5). In this density region, each PL peak is well fitted by a Lorentzian function, which means that homogeneous broadening dominates the PL linewidths. As the carrier density was further increased above 6×10^5 up to 1.2×10^6 cm^{-1}, the S-peak gradually became asymmetric in shape and dominated the wire PL.

The corresponding mean distance r_s is from $8a_B^*$ at 1×10^5 cm^{-1} to $0.7a_B^*$ at 1.2×10^6 cm^{-1}. In such a high density region, excitons start overlapping with each other and the interactions between them increase with the e–h pair density. Indeed, the exciton PL peak and the S-peak rapidly increased in linewidth, indicating significant increases in many-body interaction effects among carriers in the wire. On the basis of the lower density picture, our interpretation is that above 1×10^5 cm^{-1}, interacting excitonic and biexcitonic states are formed and their interaction strength increases, and at 6×10^5 cm^{-1} the interacting states completely change to the 1D e–h plasma. Saturation of the wire PL at higher excitation powers in Fig. 6 indicates Fermi filling of the wire electronic states, and supports the formation of degenerate e–h plasma in the wire. Note that the 1D e–h plasma peak appears at the energy position of the biexciton peak and shows small peak shifts of no more than 1 meV.

At higher excitation powers, above 0.2 mW, where the intensity and the linewidth of the wire PL were saturated, the peak position of the wire showed a red-shift up to 4 meV from the peak position of biexcitons (Fig. 8). The reason for this peak shift after complete Fermi filling of the wire states is not clear at present, but could be due to interactions with the increasing number of carriers in the arm well.

E. PL of 1D-exciton band edge

The excitation power dependence of the PL spectra from the wire at 30 K is shown in Fig. 9. For low excitation powers at 30 K, we observed not only strong PL from the ground state of 1D excitons at 1.582 eV (labeled *ground*) but also a small PL peak at 1.589 eV (labeled *excited*) and a continuous PL band with an onset at 1.593 eV (labeled *onset*). The new small peak is due to an excited state of the excitons and the continuous band is due to higher excited states of the excitons and 1D continuum states. These assignments were previously achieved by detailed PLE and absorption measurements and numerical calculations.[29,30,33]

In the PL spectra for higher excitation powers, it is remarkable that the *excited*-exciton peaks and the *onset* of the continuum states show no shift from their initial positions. This is still the case when the pair density is as high as 2×10^5 cm^{-1} ($r_s = 4a_B^*$), where the linewidth of the S-peak has already started broadening. This is crucially important and could be a key criterion in the comparison with theory, which we discuss later. At the highest pair density, 1.2×10^6 cm^{-1} ($r_s = 0.7a_B^*$), these excited-state features become smeared and buried in the tail of the broad plasma PL. However, they stay at the same energies as long as they are visible. This suggests that dense carriers contribute more effectively to scattering that broadens energy levels than to screening and self-energy change that reduce exciton binding energy in the quantum wire.

Energy positions of the PL peaks (exciton, S-peak, and exciton *excited* states) and the continuum-state *onset* observed at 5 K and 30 K are summarized all together in Fig. 10 as a function of the 1D e–h pair density n_{1D}. The origin of the vertical axis is the measured continuum-state *onset* energy (E_{g0}^*) in the low e–h density limit. The measured energy difference between the peak (or *onset*) energy (E) at each density n_{1D} and the continuum-state *onset* energy (E_{g0}^*) normalized with the measured energy difference ($E_b^* = 11.4$ meV) between the ground-state exciton and the continuum-state *onset* in the low e–h density limit is plotted.[39] Relative size of the two symbols for the exciton (closed circles) and S-peak (closed diamonds) at 5 K at each density n_{1D} approximately represents relative intensity ratio of PL peaks. Vertical bars represent FWHMs of PL peaks. As seen in Fig. 10, the broad plasma PL observed at high pair densities above 6×10^5 cm^{-1} does not continuously connect to the PL of the continuum band-edge *onset* observed as ionized states of excitons in the low density limit. Instead, it continuously begins at the energy position of biexcitons observed as S-peak in the intermediate density region. Hence, the level crossing between the continuum band edge and the exciton expected in the exciton Mott transition was not observed. In addition, at the e–h pair density of 2×10^5 cm^{-1}, PL of the continuum band edge seemed to coexist with that of the plasma as seen in Fig. 9.

IV. DISCUSSION

We first comment on the inhomogeneous broadening caused by interface roughness in the T-wire structure. In the low e–h density region, we observed a single and spatially uniform PL peak with a linewidth of 1.3 meV. This value is much larger than the probable homogeneous broadening of 1D excitons of the order of 0.1 meV. This finite linewidth of 1.3 meV and the finite Stokes shift of 0.3 meV most likely come from the thickness fluctuation of the stem well.[40] Therefore, the PL obtained in the low carrier density region was not from a single quantum state of a 1D exciton but from an ensemble of 1D exciton states. However, at high e–h densities, above n_{1D} of 1×10^5 cm^{-1}, the PL peak became broader than the inhomogeneous broadening, which indicates that the homogeneous broadening due to many-body interactions between carriers dominates the PL linewidth, and inhomogeneous broadening plays only a minor role. Therefore, at the intermediate and high densities above n_{1D} of 1×10^5 cm^{-1} of interest to us, many-body effects inherent in 1D e–h systems predominantly appeared in the spectra.

In discussing many-body effects of 1D e–h systems in quantum wires, we should take into account the finite lateral size of the quantum wires. As shown in Fig. 1, the T wire consists of two QWs (stem and arm wells) with finite well widths, which means that the e–h system formed in the T wire is not a pure 1D e–h system but a quasi-1D system. However, the quasi-1D e–h system with strong carrier confinement whose lateral size is similar or smaller than the Bohr radius of excitons, can theoretically be treat as a pure 1D system with a modified (and screened) Coulomb potential.[7,41] This is true for the T wire in this study. We should also consider the carrier-induced effects from higher-dimensional structures (stem and arm wells in the T wire) closely surrounding quantum wires. In this experiment, the excitation light created e–h pairs in the arm well and the wire but not in the stem. At low excitation powers and a low temperature, most of the photo-generated carriers in the arm well flow into the T wire and hence the carrier population in the arm well is negligible. However, at high excitation powers such that the arm-well states are filled with carriers, quasi-1D screened Coulomb potentials for the carriers in the T wire might be modified by 2D carriers existing in the arm well. Indeed, at higher excitation powers, above 0.2 mW where the wire states are almost filled and the Fermi filling has started in the arm well, the wire PL peak shows large red-shift of the peak position and broadening of the linewidth. Since the 1D e–h pair densities around and below the exciton Mott density we focus on in this work is well below the saturation density of 1.2×10^6 cm^{-1}, discussions on the 1D exciton–plasma crossover in the T wire based on the theoretical predictions for 1D e–h systems are appropriate.

Several theoretical papers have investigated 1D e–h systems during the crossover from a dilute exciton gas to a dense e–h plasma at low temperatures.[3–7] Calculations by Rossi and Molinari showed that e–h Coulomb correlation removes the 1D band-edge singularity in the optical response of an e–h plasma and theoretically showed the constancy of the excitonic peak position in optical spectra during the exciton–plasma crossover.[3] Tassone and Piermarocchi investigated strong e–h Coulomb correlation effects on scattering, which are relevant even at a high e–h density and demonstrated gradual broadening of the excitonic peak during the exciton–plasma crossover.[5] Das Sarma and Wang made self-consistent Green's-function calculations including dynamical screening in comparison with more simplified theoretical models.[7]

Optical spectra obtained as a function of the e–h density showed that the critical density separating the exciton and plasma regimes was about 3×10^5 cm^{-1}. These calculated features agree well with our present observation of the exciton-plasma crossover, but there are some important differences.

Firstly, the papers by Das Sarma and Wang give plots of the calculated 1D continuum band edge and exciton energies for various e–h densities, which demonstrate red-shifts of the band-edge energy, no shift of the exciton energy, and hence a reduction of the exciton binding energy. As a result, the constancy of the excitonic peak energy was explained as a cancellation between the band gap shrinkage and the reduced exciton binding energy. The critical density where the exciton binding energy becomes zero and the exciton level crosses the 1D continuum band edge is interpreted as the Mott density, or the critical density of the exciton Mott transition. This picture is very popular and has been also mentioned in the other papers. However, such a plot does not agree with our present observation summarized in Fig. 10. In our experiments, the 1D continuum band edge was not shifted, at least in the range up to 2×10^5 cm^{-1}, while the calculation predicts a red-shift of 15 meV or more at this density.[7] Furthermore, our experiment found no shift of the 1D continuum band edge as far as it was visible. There is no experimental evidence for level crossing between excitons and the 1D continuum band edge. Therefore, our experiment does not give any well-defined critical density or critical point for the exciton Mott transition. These discrepancies at least suggest the need to reconsider the prevailing picture of the exciton Mott transition in 1D e–h systems.

Secondly, all the above theories neglected the spins of electrons and holes, and hence neglected biexcitons. However, our present experiment shows that spins, or biexciton effects, are very important. In fact, the plasma PL band was continuously formed from the biexciton PL peak as a result of increased intensity and broadened width. The energy of the plasma PL stayed centered at the peak of biexciton PL.

The importance of the biexciton correlations in dense 1D e–h systems has been shown by Asano and Ogawa.[42] They theoretically studied dense 1D e–h systems correlated through long-range Coulomb interactions by using the Tomonaga-Luttinger model. In that paper, they found that at absolute zero temperature, the system is an insulator even in the high e–h density regime and exhibits strong instability toward the biexciton crystallization. They also predicted that, even at a finite temperature, the biexciton correlation would dominate the other correlation effects and that the system would have the character of a biexciton liquid. In short, the 1D e–h plasma with Coulomb interactions should have strong biexciton correlations. Our experimental result that the e–h plasma emission appeared gradually at the energy position of the biexciton emission, indicating the importance of the biexciton correlations, is consistent with this theoretical result. This theory assumes a mathematical model of a 1D e–h system. The inclusion of spins, or biexciton effects, in many-body theories during the exciton–plasma crossover in realistic 1D e–h systems is a very important subject of future study.

Finally, we comment on the biexciton binding energy of the T wire, E_b^{xx}. The value that we obtained was 2.8 meV, which is larger than values previously reported for other kinds of quantum wires.[14,15] The exciton binding energy E_b of this T wire was 14 meV, as characterized in our previous paper.[30] Thus, the ratio of the biexciton binding energy to the exciton binding energy (E_b^{xx}/E_b) was 0.2. An earlier theoretical work without the inclusion of excitonic polarization and deformation effects predicted E_b^{xx}/E_b of about 0.1 for a quantum wire of similar size[43]. However, recent calculations using quantum Monte Carlo methods report E_b^{xx} of 2 to 3 meV and E_b^{xx}/E_b close to 0.2 for quantum wires,[44] which is consistent with our result. Langbein *et al.* also reported the experimentally obtained biexciton binding energy for a T wire.[45] They obtained E_b^{xx} of 2 meV for a T wire that was 24 nm $\times$ 6.6 nm in size and surrounded by $Al_{0.3}Ga_{0.7}As$ barriers with E_b of 12 meV. Since our T wire was smaller and surrounded by higher-Al-content barriers, the larger biexciton binding energy that we obtained is reasonable. Reasons for the difference in biexciton binding energies between V and T wires may relate to differences in localization[46] and/or confinement structures such as lateral confinement width and strength.

V. CONCLUSION

We investigated PL spectral evolution with the e–h density in a single T-shaped quantum wire with the current-best quality by means of micro-PL spectroscopy. By using the spectrograph imaging method for the micro-PL experiments, we obtained carrier-density-dependent PL spectra for the 1D e–h system in the T wire for a wide range of e–h pair densities from 5×10^1 to 1.2×10^6 cm^{-1}.

The PL spectra from the wire reveal that the transition from excitons to an e–h plasma is a gradual crossover via biexcitons in the 1D e–h system. In the low e–h density region, PL from only excitons was observed. At a pair density of 4×10^3 cm^{-1}, the PL was characteristic of biexcitons shifted below the exciton peak by the 2.8-meV biexciton binding. At a pair density of 1×10^5 cm^{-1}, the biexciton peak broadened without an energy shift and completely changed to an e–h plasma at a density of 6×10^5 cm^{-1}. The gradual appearance of the e–h plasma peak from the biexciton peak indicates the importance of biexcitonic correlations in 1D e–h systems. Moreover, during the continuous exciton–plasma crossover, the 1D continuum band edge showed no significant energy shift at a density as high as 2×10^5 cm^{-1}, where the biexciton PL peak had already started broadening in linewidth and changing to a degenerate e–h plasma peak. Experimen-

tal evidence for the level crossing between the continuum band edge and the exciton does not exist, which doubts the existence of an abrupt metal–insulator phase transition, or exciton Mott transition, in the 1D e–h system.

VI. ACKNOWLEDGEMENTS

We thank Professor T. Ogawa, Professor K. Asano, and Dr. P. Huai (Osaka University) for valuable discussions and suggestions. This work was partly supported by a Grant-in-Aid from the Ministry of Education, Culture, Sports, Science and Technology, Japan.

* Also at Bell Laboratories, Lucent Technologies.
[1] H. Haug and S. W. Koch, *Quantum Theory of the Optical and Electronics Properties of Semiconductors*, 4th ed. (World Scientific, Singapore, 2004).
[2] C. F. Klingshirn, *Semiconductor Optics*, (Springer-Verlag, Berlin, 1997).
[3] F. Rossi and E. Molinari, Phys. Rev. Lett. **76**, 3642 (1996).
[4] E. H. Hwang and S. Das Sarma, Phys. Rev. B **58**, R1738 (1998).
[5] F. Tassone and C. Piermarocchi, Phys. Rev. Lett. **82**, 843 (1999).
[6] C. Piermarocchi, R. Ambigapathy, D. Y. Oberli, E. Kapon, B. Deveaud, and F. Tassone, Solid State Commun. **112**, 433 (1999).
[7] S. Das Sarma and D. W. Wang, Phys. Rev. Lett. **84**, 2010 (2000); D. W. Wang and S. Das Sarma, Phys. Rev. B **64**, 195313 (2001).
[8] R. Cingolani, R. Rinaldi, M. Ferrara, G. C. La Rocca, H. Lage, D. Heitmann, K. Ploog, and H. Kalt, Phys. Rev. B **48**, 14331 (1993).
[9] W. Wegscheider, L. N. Pfeiffer, M. M. Dignam, A. Pinczuk, K. W. West, S. L. McCall, and R. Hull, Phys. Rev. Lett. **71**, 4071 (1993).
[10] R. Ambigapathy, I. Bar-Joseph, D. Y. Oberli, S. Haacke, M. J. Brasil, F. Reinhardt, E. Kapon, and B. Deveaud, Phys. Rev. Lett. **78**, 3579 (1997).
[11] F. Vouilloz, D. Y. Oberli, F. Lelarge, B. Dwir, and E. Kapon, Solid State Commun. **108**, 945 (1998).
[12] J. Rubio, L. Pfeiffer, M. H. Szymanska, A. Pinczuk, S. He, H. U. Baranger, P. B. Littlewood, K. W. West, and B. S. Dennis, Solid State Commun. **120**, 423 (2001).
[13] A. Crottini, J. L. Staehli, B. Deveaud, X. L. Wang, and M. Ogura, Phys. Rev. B **63**, 121313(R) (2001).
[14] A. Crottini, J. L. Staehli, B. Deveaud, X. L. Wang, and M. Ogura, Solid State Commun. **121**, 401 (2002).
[15] T. Guillet, R. Grousson, V. Voliotis, M. Menant, X. L. Wang, and M. Ogura, Phys. Rev. B **67**, 235324 (2003).
[16] H. Akiyama, L. N. Pfeiffer, M. Yoshita, A. Pinczuk, P. B. Littlewood, K. W. West, M. J. Matthews, and J. Wynn, Phys. Rev. B **67**, 041302(R) (2003).
[17] H. Haug and S. Schmitt-Rink, Prog. Quant. Electr. **9**, 3 (1984); S. Schmitt-Rink, D. S. Chemla, and D. A. B. Miller, Adv. Phys. **38**, 89 (1989); R. Cingolani and K. Ploog, *ibid.* **40**, 535 (1991).
[18] F. Stern, Phys. Rev. Lett. **18**, 546 (1967).
[19] J. Lee and H. N. Spector, J. Appl. Phys. **57**, 366 (1985).
[20] J. A. Reyes and M. del Castillo-Mussot, Phys. Rev. B **57**, 9869 (1998).
[21] S. Benner and H. Haug, Europhys. Lett. **16**, 579 (1991).
[22] H. F. Hess, E. Betzig, T. D. Harris, L. N. Pfeiffer, and K. W. West, Science **264**, 1740 (1994).
[23] J. Hasen, L. N. Pfeiffer, A. Pinczuk, S. He, K. W. West, and B. S. Dennis, Nature **390**, 54 (1997).
[24] A. Zrenner, L. V. Butov, M. Hagn, G. Abstreiter, G. Böhm, and G. Weimann, Phys. Rev. Lett. **72**, 3382 (1994).
[25] K. Brunner, G. Abstreiter, G. Böhm, G. Tränkle, and G. Weimann, Phys. Rev. Lett. **73**, 1138 (1994).
[26] Q. Wu, R. D. Grober, D. Gammon, and D. S. Katzer, Phys. Rev. B **62**, 13022 (2000).
[27] E. Dekel, D. Gershoni, E. Ehrenfreund, D. Spektor, J. M. Garcia, and P. M. Petroff, Phys. Rev. Lett. **80**, 4991 (1998).
[28] M. Yoshita, N. Kondo, H. Sakaki, M. Baba, and H. Akiyama, Phys. Rev. B **63**, 075305 (2001).
[29] H. Akiyama, M. Yoshita, L. N. Pfeiffer, and K. W. West, Appl. Phys. Lett. **82**, 379 (2003).
[30] H. Itoh, Y. Hayamizu, M. Yoshita, H. Akiyama, L. N. Pfeiffer, K. W. West, M. H. Szymanska, and P. B. Littlewood, Appl. Phys. Lett. **83**, 2043 (2003).
[31] Y. Hayamizu, M. Yoshita, S. Watanabe, H. Akiyama, L. N. Pfeiffer, and K. W. West, Appl. Phys. Lett. **81**, 4937 (2002).
[32] M. Yoshita, Y. Hayamizu, H. Akiyama, L. N. Pfeiffer, and K. W. West, Physica E **21**, 230 (2004).
[33] Y. Takahashi, Y. Hayamizu, H. Itoh, M. Yoshita, H. Akiyama, L. N. Pfeiffer, and K. W. West, Appl. Phys. Lett. **86**, 243101 (2005).
[34] L. N. Pfeiffer, K. W. West, H. L. Störmer, J. P. Eisenstein, K. W. Baldwin, D. Gershoni, and J. Spector, Appl. Phys. Lett. **56**, 1697 (1990).
[35] A. R. Gõni, L. N. Pfeiffer, K. W. West, A. Pinczuk, H. U. Baranger, and H. L. Stormer, Appl. Phys. Lett. **61**, 1956 (1992).
[36] M. Yoshita, H. Akiyama, L. N. Pfeiffer, and K. W. West, Jpn. J. Appl. Phys. **40**, L252 (2001).
[37] M. Yoshita, H. Akiyama, L. N. Pfeiffer, and K. W. West, Appl. Phys. Lett. **81**, 49 (2002).
[38] M. Yoshita, H. Akiyama, T. Someya, and H. Sakaki, J. Appl. Phys. **83**, 3777 (1998).
[39] Since the excited exciton states due to higher Rydberg states and higher hole-subbands exist at the 1D continuum band edge, the measured continuum *onset* energy E^*_{g0} and the measured energy difference E^*_b (= 11.4 meV) are smaller than the expected 1D band-edge energy E_{g0} and the exciton binding energy E_b (= 14 meV), respectively, but are close to and represent them ($E^*_{g0} \sim E_{g0}$ and $E^*_b \sim$

E_b).
[40] One monolayer thickness difference in the (001) stem well causes an energy shift of 0.28 meV for the ground state of the T wire.
[41] T. Ogawa and T. Takagahara, Phys. Rev. B **43**, 14325 (1991); *ibid.* **44**, 8138 (1991).
[42] K. Asano and T. Ogawa, J. Lumin. **112**, 200 (2005).
[43] L. Banyai, I. Galbraith, C. Ell, and H. Haug, Phys. Rev. B **36**, 6099 (1987).
[44] T. Tsuchiya Int. J. Mod. Phys. B, **15**, 3985 (2001).
[45] W. Langbein, H. Gislason, and J. M. Hvam, Phys. Rev. B **60**, 16667 (1999).
[46] A. Feltrin, F. Michelini, J. L. Staehli, B. Deveaud, V. Savona, J. Toquant, X. L. Wang, and M. Ogura, Phys. Rev. Lett. **95**, 177404 (2005).

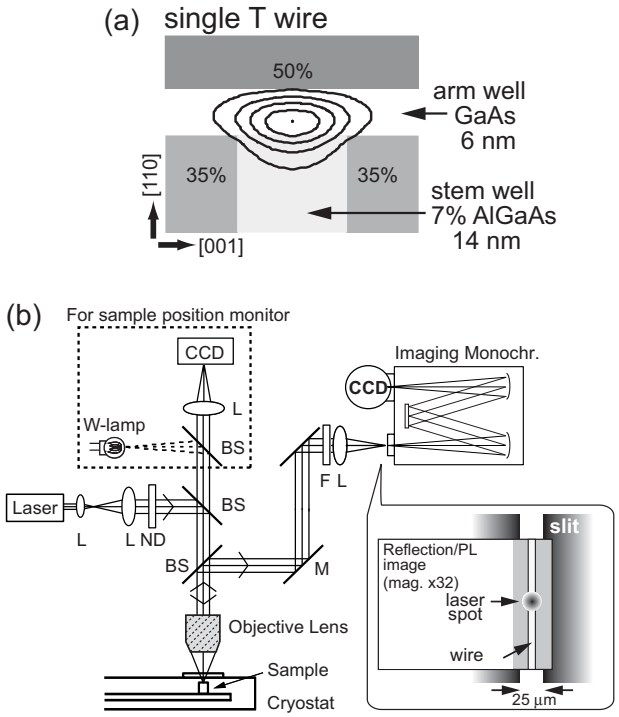

FIG. 1: (a) Schematic of a single T-wire structure. Percentages show aluminum content x in $Al_xGa_{1-x}As$ layers. (b) Micro-photoluminescence (micro-PL) setup used for PL spectrograph experiments. PL from the sample was collected by an objective lens and imaged on the entrance slit of the imaging monochromator by aligning the wire parallel to the slit. The PL image dispersed by the monochromator was detected by a liquid-nitrogen-cooled charge-coupled device (CCD) detector.

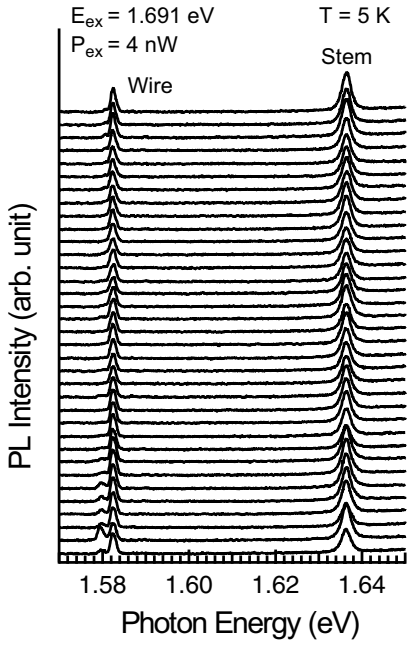

FIG. 2: Spatially resolved PL spectra of the T wire at 5 K under point excitation scanned along the wire in steps of 0.5 μm.

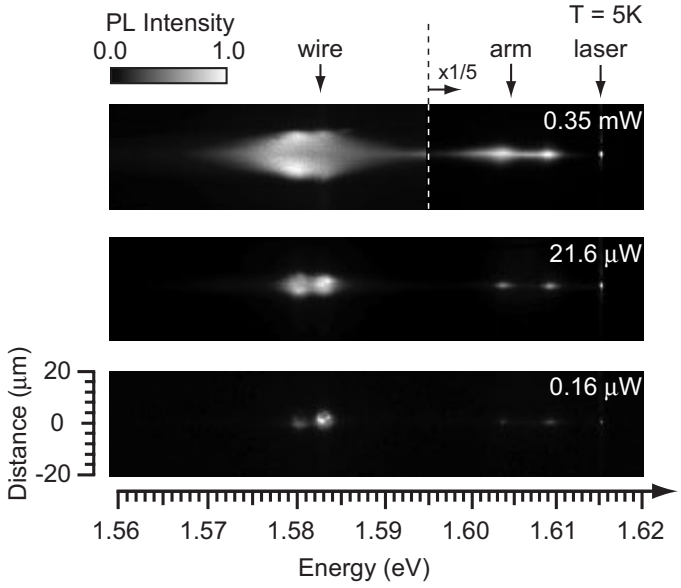

FIG. 3: Spectrograph PL images of the T wire at three different excitation powers at 5 K. Tiny spots seen at 1.6146 eV are reflection images of the excitation laser

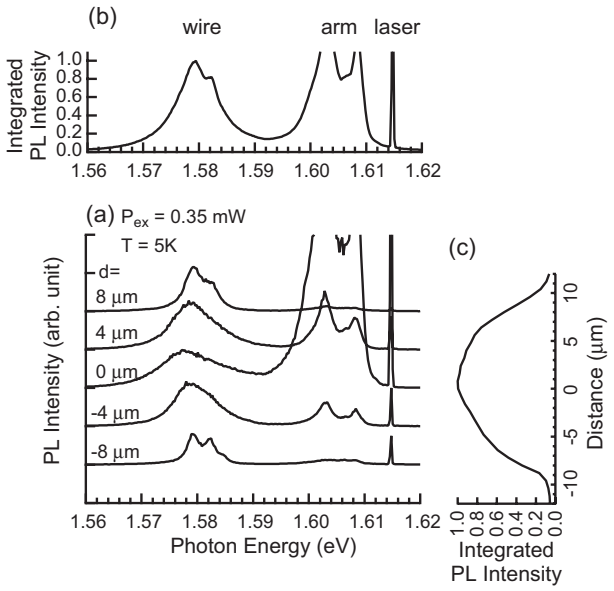

FIG. 4: (a) PL spectra of the wire at different positions, derived from the 0.35-mW spectrograph PL image in Fig. 3. (b) PL spectrum integrated over all the rows of the 0.35-mW spectrograph image in Fig. 3 along the wire direction. (c) Intensity profile of the wire PL along the wire direction, obtained by summing the PL intensities of the wire between 780 and 790 nm.

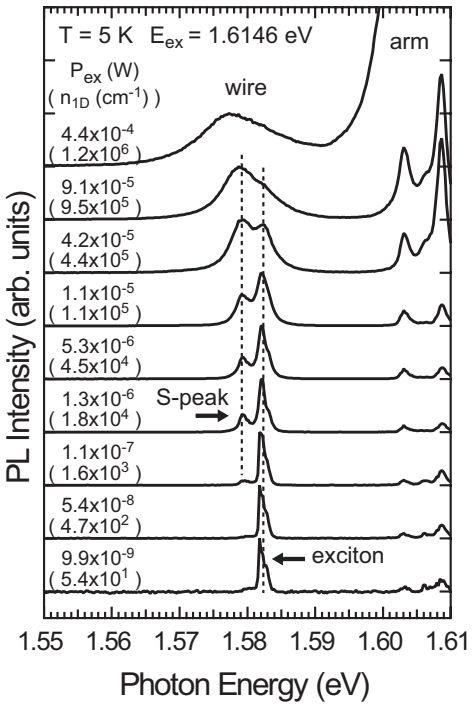

FIG. 5: Normalized PL spectra of the T wire for various excitation powers (P_{ex}) at 5 K. Numbers in parentheses are estimated 1D e–h pair densities (n_{1D}). The low-energy side peak that appeared below the wire exciton peak is labeled as the S-peak. Two dashed vertical parallel lines are drawn to guide the eyes. PL peaks observed above 1.60 eV were from the arm wells.

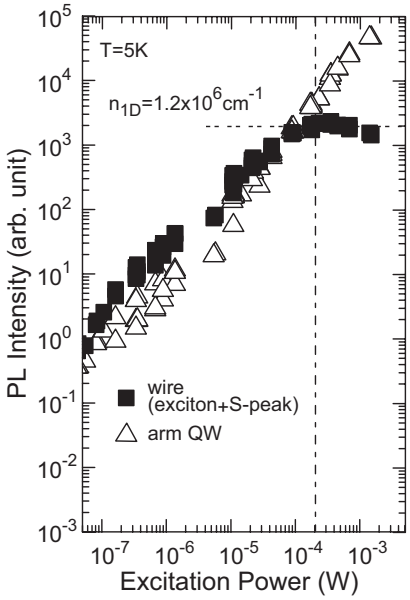

FIG. 6: Integrated intensities of PL from the wire (closed squares) and the arm well (open triangles) as a function of the excitation power. The PL intensity of the wire was saturated above the excitation power of 0.2 mW.

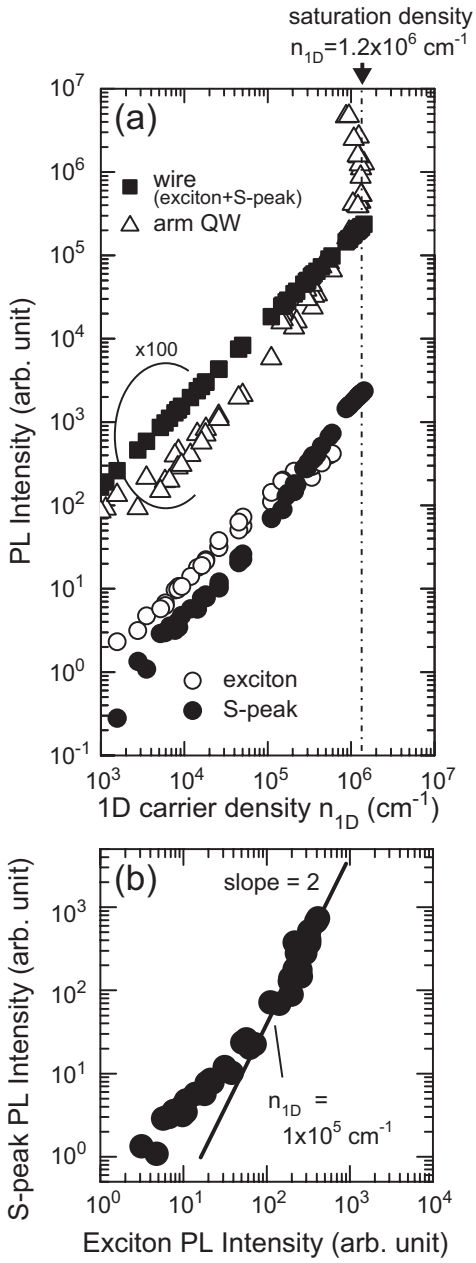

FIG. 7: (a) Integrated intensities of PL from the wire (closed squares) and the arm well (open triangles) plotted as a function of the estimated 1D carrier density n_{1D}. PL intensities of the exciton (open circles) and S-peak (closed circles) constituting the wire PL are also shown. (b) Log-log plots of the integrated PL intensity of the S-peak against that of the exciton peak.

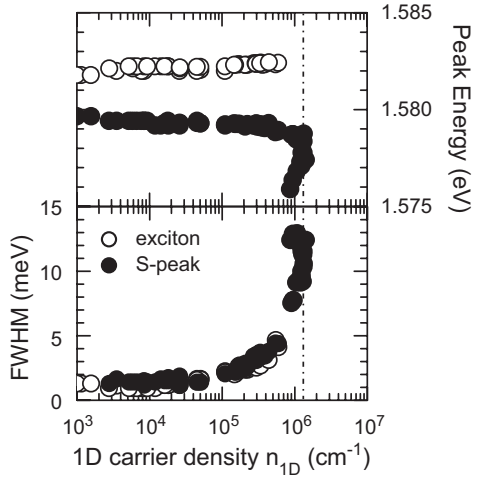

FIG. 8: Energy positions and widths of the exciton peak and S-peak in the wire PL spectra shown in Fig. 5 as a function of the 1D carrier density n_{1D}.

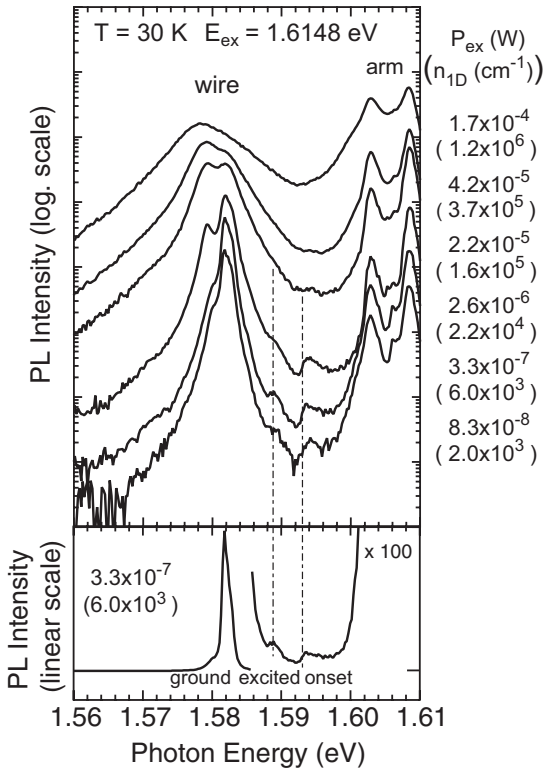

FIG. 9: (a) Excitation power dependence of PL spectra from the T wire at 30 K on a log scale. The PL spectrum at P_{ex} of 3.3×10^{-7} W is also given on a linear scale at the bottom.

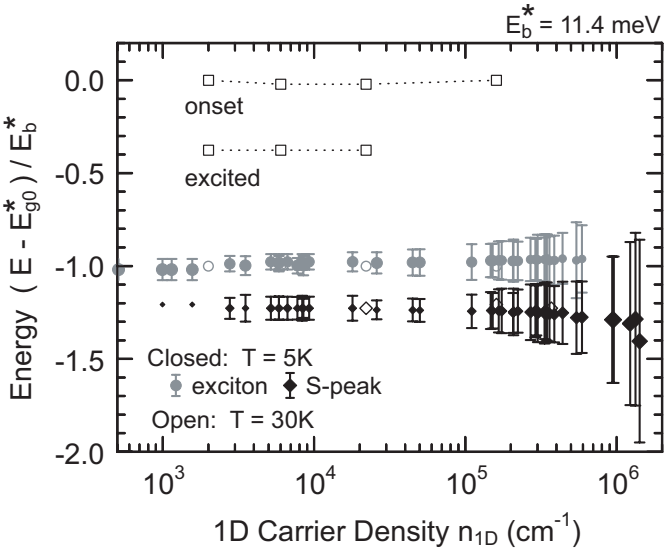

FIG. 10: Energy positions of the PL peaks (exciton, S-peak, and exciton *excited* states) and the continuum-state *onset* observed at 5 K (closed symbols) and 30 K (open symbols) as a function of the 1D e–h pair density n_{1D} in the wire. The origin of the vertical axis is the measured continuum-state *onset* energy (E^*_{g0}) in the low e–h density limit. The energy difference between the measured peak (or *onset*) energy (E) at each density n_{1D} and the continuum-state *onset* energy (E^*_{g0}) normalized with the measured energy difference (E^*_b = 11.4 meV) between the ground-state exciton and the continuum-state *onset* in the low e–h density limit is plotted. Relative size of the two symbols for the exciton and S-peak at 5 K approximately represents relative intensity ratio of PL peaks at each density n_{1D}. Vertical bars represent FWHMs of PL peaks.